FREQUENCY SCAN FOR TIME-OF-ECHO COMPRESSION IN SAR SYSTEMS

M. Younis, F. de Almeida, M. Villano, T. Bollian,G. Krieger, and A. Moreira

German Aerospace Center (DLR), Oberpfaffenhofen, Germany

1. INTRODUCTION

The development of synthetic aperture radar (SAR) instruments at higher carrier frequency is motivated, among others, by the relative wavelength scaling, which provides an increased bandwidth and reduced physical dimensions of the RF hardware, for the same coverage. The later causes a reduced area and a high length-to-height aspect ratio of the antenna, which is unfavorable, since the resulting design compromise leads to systems of small swath width and low signal-to-noise ratio.

The frequency Scan for Time-of-Echo Compression (STEC) technique described in this paper is known from [1, 2, 3] and utilizes the available bandwidth to form a narrow frequency-scanning antenna beam illuminating the swath of interest from far to near range. The operation parameters of the technique may be chosen to significantly reduce the pulse echo duration which may be used to significantly increase the transmit pulse duty cycle over what is common for SAR instruments allowing for a lower peak-to-average transmitted power ratio.

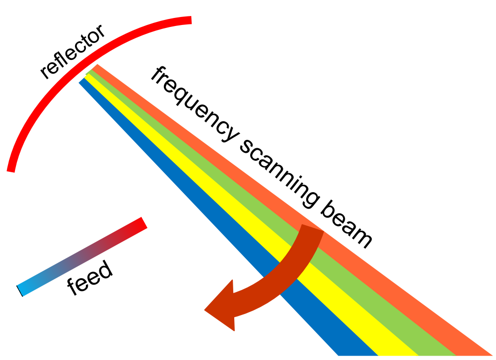

Fig. 1. The frequency scan operation technique as realized for a reflector SAR system.

The paper provides a simple model describing STEC operation modes. It is shown that the technique trades range resolution for signal-to-noise ratio, azimuth resolution, and swath width. The technique is shown to be especially favorable for high carrier frequency SAR systems.

The technique is especially suitable for spaceborne SAR systems operating at high frequencies, where other advanced digital beam-forming techniques may not be available due to technology limitations. The performance metric of the technique is derived, and a comparison to classical stripmap operation mode shows an improvement of several decibels.

2. OPERATION PARAMETERS

In the following we proceed by developing equations that describe the mode parameters assuming ideal, i.e. simplified, conditions and by this accentuating the trade space. Although the developed equations may be used to provide quantitative instrument design parameter values the approached followed here is comparative in the sense that the values and the performance are compared to a conventional SAR operating in stripmap mode (the comparison will be later extended to include a more advanced digital beam-forming SAR operating in SCan-On-REceive mode).

2.1. Dwell Bandwidth and Dwell Time

The main two parameters are the dwell bandwidth and the dwell time which are defined as the duration during which a point target is illuminated by a single radar transmit pulse and the range of frequencies (bandwidth) seen by the point target during that time, respectively. The mathematical expressions of these two parameters can be derived without taking the *continuous* beam scanning into account; instead an equivalent system illuminating the swath by a finite set of *fixed* antenna beams is considered, where each beam is active during a fraction of the transmit chirp pulse duration and thus occupies a fraction of the available bandwidth.

The antenna beamwidth in elevation, Θ_{el}, is, for simplicity, assumed to be independent of the scan angle and given by:

$$\Theta_{el} = \gamma_{el} \frac{\lambda}{h_{ant}} \quad (1)$$

where λ is the carrier wavelength; h_{ant} the antenna height (in cross-track direction); and γ_{el} a constant of proportionality which depends mainly on the antenna type, taper and illumination. The angular swath extent is denoted by Θ_{sw}, while the available signal bandwidth is B_w. Since the direction (i.e. scan angle) of the antenna's main beam is determined by the signal frequency, there is a one-to-one correspondence between the instantaneous frequency and the beam scan angle. Transmitting a linearly frequency modulated signal (known as chirp) thus causes the main beam scan angle to vary with time.

A closed expression for the dwell bandwidth —which determines the range resolution— can then derived to be:

$$B_{dwell} = \frac{B_w}{\frac{\Theta_{sw}}{\Theta_{el}} + 1}. \quad (2)$$

where Θ_{sc} is the angular scan extent being larger than the angular swath extent by an amount equal to the antenna beamwidth.

The trade-space described by (2) is shown in Fig. 2. The left ordinate represents the relative dwell bandwidth, B_{dwell}/B_w in percent versus the abscissa taken to be the STEC antenna height normalized to the height of a stripmap SAR antenna imaging the same swath. Increasing the antenna height –beneficial, as it increases the antenna gain– reduces the antenna beamwidth and by this the spectral support of a point target positioned within the swath.

The right ordinate of Fig. 2 represents the swath-to-beamwidth ratio, Θ_{sw}/Θ_{el}, introduced earlier. The line has a slope of 1 for identical STEC and stripmap antenna types.

The closed expression for the dwell time is derived in terms of the transmit pulse duration τ_p to be:

$$\tau_{dwell} = \frac{\tau_p}{\frac{\Theta_{sw}}{\Theta_{el}} + 1}. \quad (3)$$

Figure 2 also shows the percentage dwell time as a function of normalized antenna height. Comparing (3) to (2) shows an identical form of dependency for the dwell time and dwell bandwidth. The implication, however, is rather different as reduced dwell bandwidth is advantageous in terms of the SNR, while the opposite is true for the dwell time, since a reduced point target illumination time reduces the average power density and by this causes a reduced SNR, cf. Section 3.

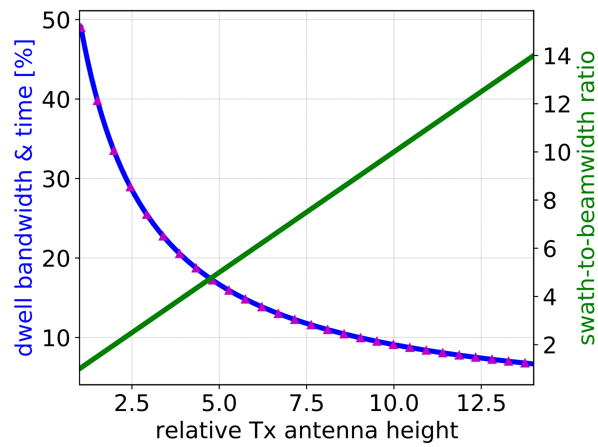

Fig. 2. Dwell bandwidth & dwell time (left ordinate) and the ratio of the angular swath extent to antenna pattern beamwidth (right ordinate) plotted versus the antenna height normalized to the height of a stripmap antenna imaging the same swath width.

2.2. Echo Time Reversal Condition

The antenna beam scans the swath from far to near range, thus directing the signal at time t_1 to the *far* range and at $t_1 + \tau_p$ to the *near* range. The scattered echo of the leading pulse edge will arrive at time instance $t_{far} = t_1 + \frac{2R_{far}}{c_0}$ while the echo of the lagging pulse edge will arrive from the near range at time $t_{near} = t_1 + \tau_p + \frac{2R_{near}}{c_0}$.

The STEC technique allows for an echo time reversal, which occurs, if the far range signal echo arrives before the near range signal echo, such that $t_{far} < t_{near}$. The condition for the minimum pulse duration to ensure echo time reversal is:

$$t_{far} < t_{near} \Rightarrow \tau_p > \frac{2}{c_0}(R_{far} - R_{near}) = \tau_0 \quad (4)$$

where the term τ_0 is named the *intrinsic duration*. The above expression conveys that a long pulse duration and a small swath width work in favor of time reversal.

When $t_{far} = t_{near}$ the system operates at the reversal point for which it will be shown that the echo window length is minimized. In general, it turns out that operating an STEC SAR in echo time reversal and near the reversal point is advantageous in terms of the performance and system resources.

2.3. Pulse Repetition Interval and Pulse Duty Cycle

A crucial parameter of SAR is the pulse repetition frequency (PRF), which is the inverse of the pulse repetition interval (PRI), i.e. $f_{PRF} = 1/T_{PRI}$. It must be ensured that the duration of the later is sufficient to accommodate the transmit pulse of duration τ_p and the echo window length T_{echo}, in addition to some margin (guard time). The minimum PRI is thus:

$$\begin{aligned} T_{PRI} &= T_{echo} + \tau_p \\ &= \begin{cases} 2\tau_p - \tau_0 + \tau_{dwell} & \text{echo reversal} \\ \tau_0 + \tau_{dwell} & \text{no echo reversal} \end{cases} \end{aligned} \tag{5}$$

where τ_0 is the intrinsic echo duration which already appeared in (4).

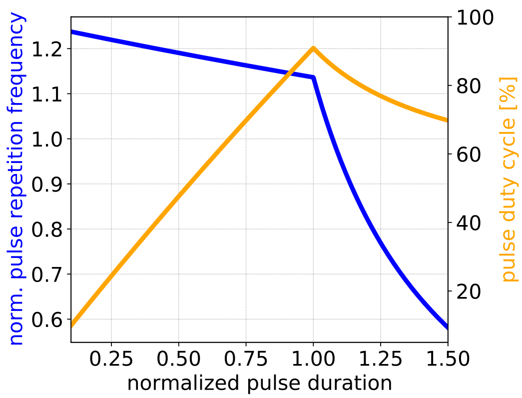

Fig. 3. Pulse repetition frequency (PRF) of STEC SAR relative to the PRF of a stripmap SAR imaging the same swath (left ordinate) and the percentage pulse duty cycle (right ordinate) plotted versus the pulse duration normalized to the intrinsic duration. The STEC system operation point is $B_{dwell} = B_w/2$ while the stripmap system pulse duty cycle is taken to be $10\,\%$.

The left ordinate in Fig. 3 shows the PRF normalized the PRF of a stripmap SAR versus the normalized pulse duration τ_p/τ_0 for the case that $B_{dwell} = B_w/2$. The reversal point is for $\tau_p = \tau_0$, thus the system operates in echo time reversal for abscissa values larger than 1. The plot shows that near the reversal point the PRF is slightly higher with respect to stripmap operation; this allows a more square-like antenna shape and a better azimuth resolution.

A further quantity of interest is the pulse duty cycle, which is the percentage of time the system is transmitting given by:

$$\begin{aligned} dc &= \frac{\tau_p}{T_{PRI}} \\ &= \begin{cases} \frac{\tau_p}{2\tau_p - \tau_0 + \tau_{dwell}} & \text{echo reversal} \\ \frac{\tau_p}{\tau_0 + \tau_{dwell}} & \text{no echo reversal} \end{cases} \end{aligned} \tag{6}$$

and the percentage duty cycle is plotted in Fig. 3 (right ordinate). The peak duty cycle is at the time reversal point and exhibits exceptionally high values in the order of $90\,\%$, much higher (about 5 to 10 times) than what is usually possible for spaceborne SAR. The high dc values allow for low peak-to-average transmit power and is believed to be a major advantage of STEC operation as it significantly reduces the complexity of the transmitter unit and allows for large transmit power thus improving the SNR, one of the main deficiencies of Ka-band spaceborne SAR.

3. SIGNAL-TO-NOISE RATIO PERFORMANCE

The increased antenna height of an STEC SAR system is expected to result in a higher signal-to-noise ratio (SNR) when compared to a conventional stripmap SAR imaging the same swath. Further, it is worth comparing the SNR to that of a digital beam-forming system utilizing SCORE.

Starting from the well-known radar equation for extended targets [4, 5] while taking the particularities of this operation mode into account results in the following expression for the SNR:

$$\begin{aligned} SNR = & \frac{P_{av}(A_e)^2}{8\pi\lambda^2} \frac{\sigma_0 c_0}{\mathrm{k} T_N B_{dwell} L_f} \frac{\Phi_{az}}{B_D R(\vartheta)^3 \sin\eta_i} \frac{\tau_{dwell}}{\tau_p} \\ & \frac{1}{\Phi_{az}} \int_{\Phi_{az}} |C_{az}(\phi)|^4 \, \mathrm{d}\phi \cdot \frac{1}{\Theta_{el}} \int_{\Theta_{el}} |C_{el}(\vartheta)|^4 \, \mathrm{d}\vartheta \end{aligned} \tag{7}$$

where P_{av} is the average transmit power, which is related to the peak power through $P_{av} = P_t \tau_p f_{PRF} = P_t dc$; A_e is the effective antenna, $A_e = \lambda^2 G/4\pi$; k is Boltzmann's constant; T_N the system noise temperature; L_f the system losses; σ_0 the backscatter coefficient; B_D the processed Doppler bandwidth; Φ_{az} and $C_{az}(\phi)$ the azimuth beamwidth and normalized radiation pattern, respectively. The last two terms in the above expression represent the azimuth power reduction factor and the two-way pulse extension loss [6]. The former takes into account, that only the power within the azimuth beamwidth Φ_{az}, which corresponds to the processed Doppler bandwidth contribute to the SNR as detailed in [4]. The later considers the loss of the two-way elevation antenna pattern within the angular pulse extent[1].

To compare SAR systems designed to operate in different modes it is necessary to define parameters common to these systems; these are taken to be the swath width ($50\,\mathrm{km}$), the average power ($100\,\mathrm{W}$), and the 2-D resolution ($5.6\,\mathrm{m}^2$); the later (product of range and azimuth resolution) affecting the processed range and Doppler bandwidth.

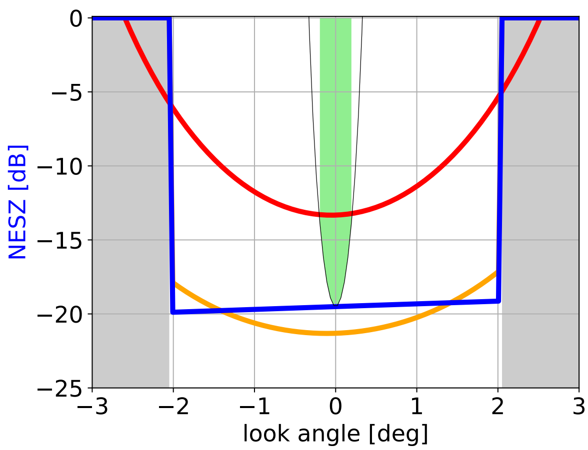

Fig. 4. Noise-equivalent sigma-zero comparison between stripmap, SCORE and STEC

The three systems are compared with respect to their Noise-Equivalent Sigma-Zero (NESZ) values, computed from the SNR according to $NESZ = \sigma_0|_{SNR=1}$, as shown in Fig. 4 versus the swath-centred look angle. The STEC system is characterized by a nearly constant NESZ over the swath which is due to the Tx/Rx beam scanning property; it clearly outperforms the stripmap system the main reason being the small antenna area of the later which further suffers from an extremely high length-to-height aspect ratio of 30. The SCORE system shows a good performance the main reason being even outperforming STEC at the swath center (roll-off at the swath boarders is due to the fixed low-gain transmit pattern). The main reason being that STEC suffers from a shorter effective point target pulse duration, cf. factor τ_{dwell}/τ_p in (7), which degrades the NESZ by a factor of 10 with respect to SCORE. Despite its good performance, the SCORE system can be considered an inferior choice at higher carrier frequencies (Ka-band and above) because of its high complexity and technology demand (multi-channel RF hardware and on-board digital processing unit). Last but not least it is noted that assuming the same average transmit power $P_{av} = 100\,\mathrm{W}$ for all three systems penalizes STEC since it does not benefit from the high pulse duty cycle of $74\,\%$.

[1] In [6] only the effect of the receive, i.e. one-way, antenna pattern within the angular pulse extent is considered, as applicable for a DBF system utilizing SCORE. For STEC the expression is modified to consider both the receive and transmit antenna patterns resulting in a $|C_{el}(\vartheta)|^4$ dependency

4. REFERENCES

[1] C. Roemer, R. Gierlich, J. Marquez-Martinez, and M. Notter, “Frequency scanning applied to wide area SAR imaging,” in *Proc. European Conference on Synthetic Aperture Radar EUSAR’2018*, Aachen, Germany, June 2018.

[2] C. Römer, “High resolution wide swath synthetic aperture radar system,” United States Patent Patent US 2020/0 174 114, June, 2020.

[3] L. Nan, G. Gai, T. Shiyang, and Z. Linrang, “Signal modeling and analysis for elevation frequency scanning HRWS SAR,” *IEEE Transactions on Geoscience and Remote Sensing*, vol. 58, no. 9, pp. 6434–6450, Sept. 2020.

[4] R. K. Raney, “SNR in SAR,” in *Proc. Int. Geoscience and Remote Sensing Symposium IGARSS’1985*, Amherst, MA, USA, Oct. 1985, pp. 994–999.

[5] M. Younis, “NESZ-formulation for planar multi-channel SAR,” German Aerospace Center, Microwaves and Radar Institute, Technical Note HR-RK-TN MY101, issue 2.3, Apr. 2019.

[6] M. Younis, T. Rommel, F. Bordoni, G. Krieger, and A. Moreira, “On the pulse extension loss in digital beamforming SAR,” *IEEE Geoscience and Remote Sensing Letters*, vol. 12, no. 7, pp. 1436–1440, July 2015.